Artificial Cells, Nanomedicine, and Biotechnology
An International Journal

ISSN: (Print) (Online) Journal homepage: informahealthcare.com/journals/ianb20

Fullerene C_{60} functionalized γ-Fe_2O_3 magnetic nanoparticle: Synthesis, characterization, and biomedical applications

Ersin Kılınç

Artificial Cells, Nanomedicine, and Biotechnology, 2016; 44: 298–304

ISSN: 2169-1401 print / 2169-141X online
DOI: 10.3109/21691401.2014.948182

Taylor & Francis
Taylor & Francis Group

Fullerene C_{60} functionalized γ-Fe_2O_3 magnetic nanoparticle: Synthesis, characterization, and biomedical applications

Ersin Kılınç

Department of Medical Laboratory Techniques, Vocational School of Healthcare Studies, Mardin Artuklu University, Mardin, Turkey

Abstract
Hybrid magnetic nanoparticles composed from C_{60} fullerene and γ-Fe_2O_3 were synthesized by hydrothermal method. XRD, FT-IR, VSM, SEM, and HR-TEM were employed for characterizations. The magnetic saturation value of C_{60}-γ-Fe_2O_3 magnetic nanoparticles was 66.5 emu g^{-1}. Concentration of Fe in nanoparticles asdetermined by ICP-OES was 40.7% Fe. Particle size of C_{60}-γ-Fe_2O_3 magnetic nanoparticles was smaller than 10 nm. Maximum adsorption capacity of C_{60}-γ-Fe_2O_3 for flurbiprofen, a non-steroidal anti-inflammatory drug, was calculated from Langmuir isotherm as 142.9 mg g^{-1}.

Keywords: biomedical application, chemical synthesis, magnetic materials, magnetic properties

Introduction

Magnetic nanoparticles (MNPs) show magnetic behavior when exposed to magnetic fields and they do not retain any magnetism once the applied magnetic field is removed. These particles have an important application area in biotechnology (Gao et al. 2009). Metallic, bimetallic, and superparamagnetic iron oxide nanoparticles (SPIONs) are classified as MNPs (Veiseh et al. 2010). Among SPIONs, γ-Fe_2O_3 and Fe_3O_4 attained special attention due to their biocompatibilities, biodegradabilities, availabilities, stabilities, and high magnetic susceptibilities (Donadel et al. 2008, Yiu and Keane 2012). Magnetic nanoparticles have been widely used for protein adsorption (Liu et al. 2004), bacterial detection and protein purification (Gao et al. 2009), targeted drug delivery (Berry and Curtis 2003), cancer diagnosis/therapy (Kievit and Zhang 2011, Yigit et al. 2012), photodynamic therapy (Huang et al. 2011), bioanalytical sensor (Stanciu et al. 2009), as supporting materials for enzymes (Netto et al. 2013). SPIONs sized between 10 and 100 nm can be used for *in vivo* and *in vitro* studies due to size similarities with biological macromolecules, cells, and enzymes (Yiu and Keane 2012). Magnetic nanoparticles could be converted to biocompatible forms by coating with poly(ethyleneglycol), dextran, chitosan, copolymers, polyethyleneimine, liposomes, and micelles for *in vivo* studies (Veiseh et al. 2010, Yigit et al. 2012). Additionally, surface coating could also significantly influence the cytotoxicities of SPIONs (Donadel et al. 2008). Surface coating increases the half-life of SPIONs in blood by reducing the adsorption of proteins onto the surfaces (Gupta and Wells 2004).

New carbon allotrope containing 60 perfectly symmetrically arranged carbon atoms (C_{60}) was discovered in 1985 and called as buckminsterfullerene (Kroto et al. 1985). The combination of the unique three-dimensional shape, physical, chemical, electrical, and optical properties with the extremely rich carbon chemistry makes fullerene one of the most exciting materials of nanobiotechnology that this field produces and investigates the nanomaterials in biotechnology and medicine. Diameter of a fullerene C_{60} molecule is 7 Å and this size makes it a potential nanomaterial for biological applications (Partha and Conyers 2009). Additionally, covalent functionalization of fullerene opens the door to various applications in the drug delivery (Brettreich et al. 2000), photodynamic cancer therapy (Mroz et al. 2007), gene delivery (Nakamura et al. 2000), antioxidant (Enes et al. 2009), magnetic resonance imaging (MRI) contrast agent (Tóth et al. 2005), and photocatalyst (Meng et al. 2012) fields. The role of functionalized fullerene in a new emerging research area, nanobiotechnology, that includes nanomedicine and biomedical applications was reviewed with details (Satoh and Takayanagi 2006, Partha and Conyers 2009). It should be noted that toxicity of functionalized fullerene is not well understood (Zhang et al. 2009). Self-assembled spherical nanostructures derived from amphiphilic fullerene were used as nanocarrier called as buckysomes for paclitaxel, a highly hydrophobic anticancer drug. It was reported that paclitaxel-embedded buckysomes demonstrated a similar efficacy to that of commerical one in cell viability studies (Partha et al. 2008). Antioxidant effects and *in vivo* radioprotective effect of a water-soluble antioxidant based on the

Correspondence: Ersin Kilinç, Department of Medical Laboratory Techniques, Vocational School of Healthcare Studies, Mardin Artuklu University, 47200 Mardin, Turkey. Tel: + 90 (482) 212 69 49-7284. E-mail: kilincersin@gmail.com

(Received 14 May 2014; revised 20 July 2014; accepted 21 July 2014)

hollow nanostructure of fullerenes derivative (dendrofullerene) containing 18 carboxylic groups was evaluated (Daroczi et al. 2006). A fullerene derivative bearing two diamino side chains bound to a plasmid vector DNA was used for nonviral gene delivery (Isobe et al. 2006). Due to its low stability and self-aggregation tendency, functionalization of fullerene is required. The water-soluble endohedral gadofullerene derivatives have found application area in MRI as contrast agent (Tóth et al. 2005).

The profen family including flurbiprofen {(R,S)-[2-(2-fluoro-4-phenyl) phenyl] propionic acid} is a member of non-steroidal anti-inflammatory (NSAI) drugs (NSAIDs) (Bae et al. 2006). Pharmacological activities of the commonly consumed NSAIDs are predominantly attributed to inhibitory effect on the activity of the cyclooxygenase (COX) enzyme catalyzing the first step in the conversion of arachidonic acid to prostaglandins and thromboxanes (Sorge et al. 1998, Hinz et al. 2001). Among available NSAI agents, flurbiprofen is the most commonly used one among others (Pignatello et al. 2002). The family exists in two stereo-isomeric forms, yet only an (S)-enantiomer exhibits pharmacological activity through the inhibition of the cyclooxygenase system while an (R)-enantiomer is not only biologically inactive but also demonstrates gastrointestinal toxicity and chiral inversion (Lee et al. 2003, Bae et al. 2006).

Therefore, new hybrid materials composed of fullerene and iron oxide would be extremely attractive. Unique properties of C_{60} and magnetic nanoparticles could be combined to increase their activities and potential biomedical applications by further investigations. In this paper, C_{60}-γ-Fe_2O_3 magnetic nanoparticle was synthesized and magnetic properties, chemical composition, surface functionalities, morphology, and micro structures of the synthesized magnetic nanoparticles were thoroughly characterized by SEM, TEM, FT-IR, ICP-OES, and vibrating sample magnetometer (VSM).

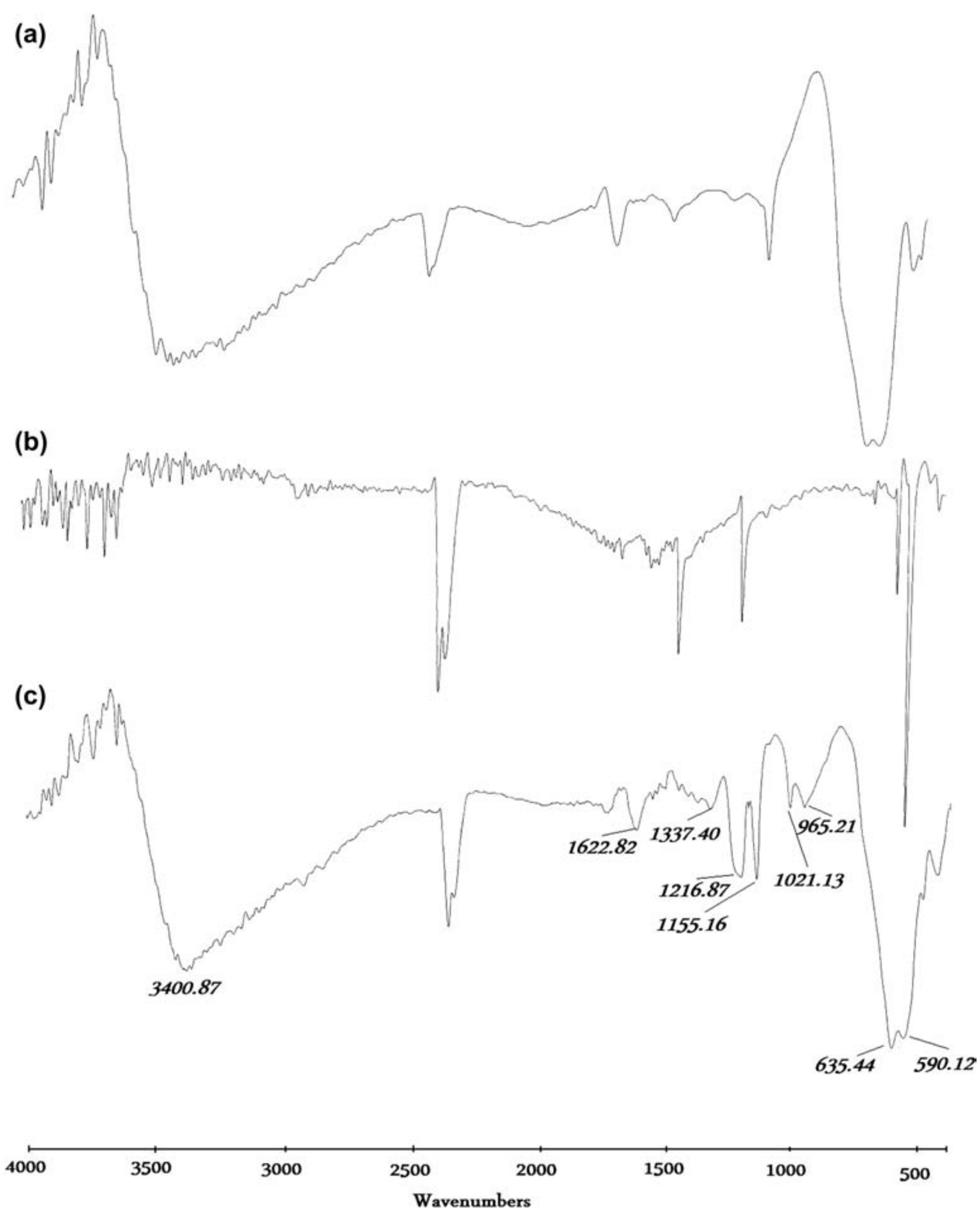

Figure 1. Comparison of FT-IR spectra of a) γ-Fe_2O_3 magnetic nanoparticle, b) C_{60}, c) C_{60}-γ-Fe_2O_3 SPIONs.

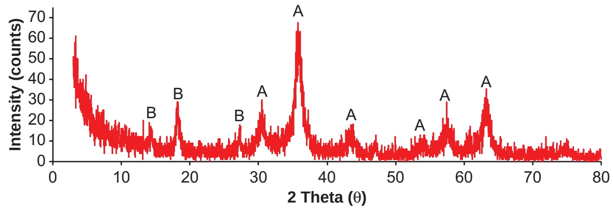

Figure 2. XRD patterns of C_{60}-γ-Fe_2O_3 SPIONs, A: peaks correspond to C_{60}, B: peaks correspond to γ-Fe_2O_3.

Materials and methods

Reagents and standards

Fullerene C_{60} (>98%), toluene, NH_4OH, flurbiprofen were supplied from Sigma-Aldrich (St. Loius, MO). $FeCl_3{\cdot}6H_2O$ and $FeCl_2$ were bought from Merck (Darmstadt, Germany). All chemicals were of analytical reagent-grade. Doubly distilled water was used throughout the experiments.

Instrumentation

Total Fe concentrations in C_{60} conjugated γ-Fe_2O_3 magnetic nanoparticle and C_{60} were determined by ICP-OES (Perkin Elmer, Optima 2100 DV) at the wavelength of 238.204 nm. Instrumentation conditions were given in our previous study (Kilinc and Aydin 2012). C_{60} residue in synthesized SPIONs was monitored by UV-VIS spectrophotometer (Perkin Elmer, Lambda 25). Infrared spectra of magnetic nanoparticle in KBr pellet were recorded in the ranges of 4000–400 cm^{-1} by Mattson Model 1000 FT-IR spectrophotometer. The Model P525 VSM measurement system (Quantum Design) for the physical property measurement system (PPMS) was used at 27°C. SEM analysis was carried out by LEO-Evo 40 XVP scanning electron microscope. HR-TEM images were recorded on Jeol JEM 2100F HRTEM instrument working at 200 kV with a probe size under 0.5 nm. Concentration of flurbiprofen was also measured by UV-VIS spectrophotometer at 250 nm (Kilinc and Aydin 2009).

Synthesis of γ-Fe_2O_3 SPIONs

Approximately 0.01 g of MNP and 0.03 g of fullerene C_{60} were weighted and placed in a beaker. Three mL of concentrated HCl and 1.0 mL of HNO_3 and 0.5 mL of H_2O_2 were added and heated until dried. Residues were dissolved in 50 mL and 5.0 mL of 1.0 M HNO_3, for C_{60} conjugated γ-Fe_2O_3 SPIONs and C_{60}, respectively. Total Fe concentrations were determined by ICP-OES. Surface functionalities were discussed by comparing their FT-IR spectra. The samples were prepared as film on KBr windows. The spectra were recorded in the transmission mode. Chemical structure of γ-Fe_2O_3 nanoparticle functionalized with fullerene C_{60} was determined by XRD. XRD traces were recorded from 2Θ of 2°–80° with a 0.02° step size. VSM was employed to determine the magnetic saturation value of C_{60}-γ-Fe_2O_3 magnetic nanoparticles

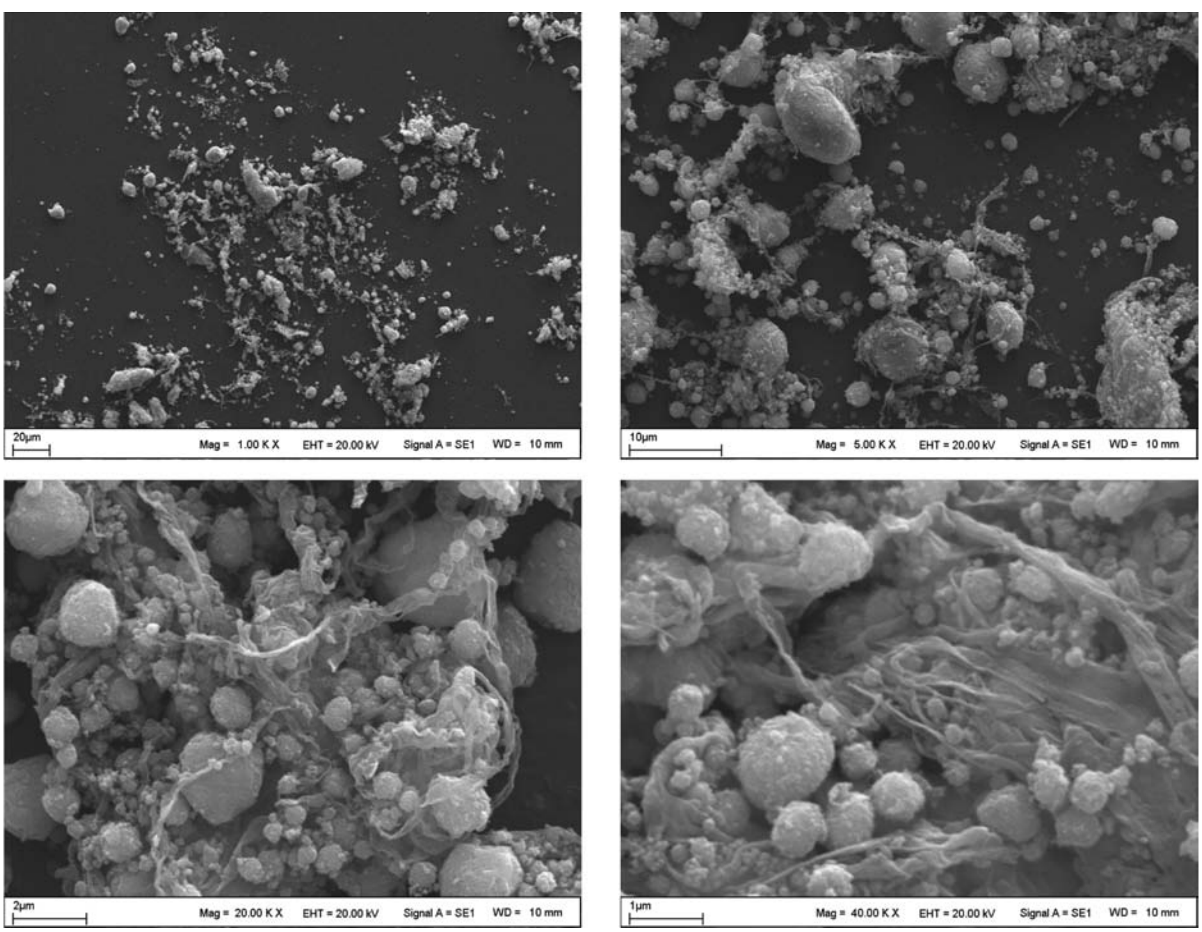

Figure 3. Comparison of SEM images of C_{60}-γ-Fe_2O_3 SPIONs.

at room temperature. SEM was used for characterization of macrostructure of nanomaterials with different resolutions. The morphology and microstructure of C_{60}-γ-Fe_2O_3 magnetic nanoparticles were investigated by HR-TEM.

Synthesis of C_{60}-γ-Fe_2O_3 SPIONs

γ-Fe_2O_3 (0.36 g) was added to the solution of 0.17 g of C_{60} fullerene dissolved in 100.0 mL of toluene. The mixture was sonicated for 5.0 min at 30°C and vigorously stirred for 3 days at room temperature. $FeCl_3.6H_2O$ and $FeCl_2$, at the molar ratio of 2:1, were dissolved in distilled water and stirred in a 100.0 mL three necked flask. 30.0 mL of 5% NH_4OH solution was added dropwise at 75°C with vigorous stirring for about 2.0 h under nitrogen purge. It was subsequently washed with distilled water, toluene, and absolute ethanol until the C_{60} absorption peak disappeared by monitoring UV-VIS spectra at 554 nm.

Adsorption of flurbiprofen on C_{60}-γ-Fe_2O_3

Adsorption of flurbiprofen on C_{60}-γ-Fe_2O_3 SPIONs was investigated. Briefly, flurbiprofen solutions at the concentration of 5.0 µg mL^{-1} were prepared in water and buffer. Twenty mg of C_{60}-γ-Fe_2O_3 SPIONs was added to it and magnetically stirred for 30 min at 100 rpm. Experiments were performed at 25°C. Then, SPIONs were removed by a strong magnet. The concentrations of flurbiprofen in remaining solutions were determined by UV-VIS spectrophotometer at 250 nm. flurbiprofen adsorbed on C_{60}-γ-Fe_2O_3 SPIONs was also released with different solvent and buffers.

Results and discussion

Characterization of C_{60} functionalized γ-Fe_2O_3 magnetic nanoparticles

Wide ranges of physical and chemical characterization are utilized in synthesizing and determining the functions of nanoparticles. Surface functionality, magnetization value and surface morphology are properties that should be considered and evaluated. Thus, C_{60}-γ-Fe_2O_3 magnetic nanoparticles were characterized by various physical and chemical techniques.

Fe concentrations in fullerene C_{60}, C_{60}-γ-Fe_2O_3 magnetic nanoparticles were determined by ICP-OES after wet digestion on hot plate by using concentrated HCl followed by mixture of HNO_3 and H_2O_2 (1:1, v/v). Fe concentration in pristine C_{60} was 847.5 mg kg^{-1} while in C_{60}-γ-Fe_2O_3 magnetic nanoparticles it was 40.8%. While Fe amount in pure γ-Fe_2O_3 was considered as 70%, it could be concluded C_{60} reacted with γ-Fe_2O_3 to give a new product of γ-Fe_2O_3 coated with C_{60}. These also confirm the coating of C_{60} on γ-Fe_2O_3.

Comparison of FT-IR spectra of γ-Fe_2O_3 magnetic nanoparticle, C_{60} and C_{60}-γ-Fe_2O_3 magnetic nanoparticles is presented in Figure 1. The wide absorption band at about

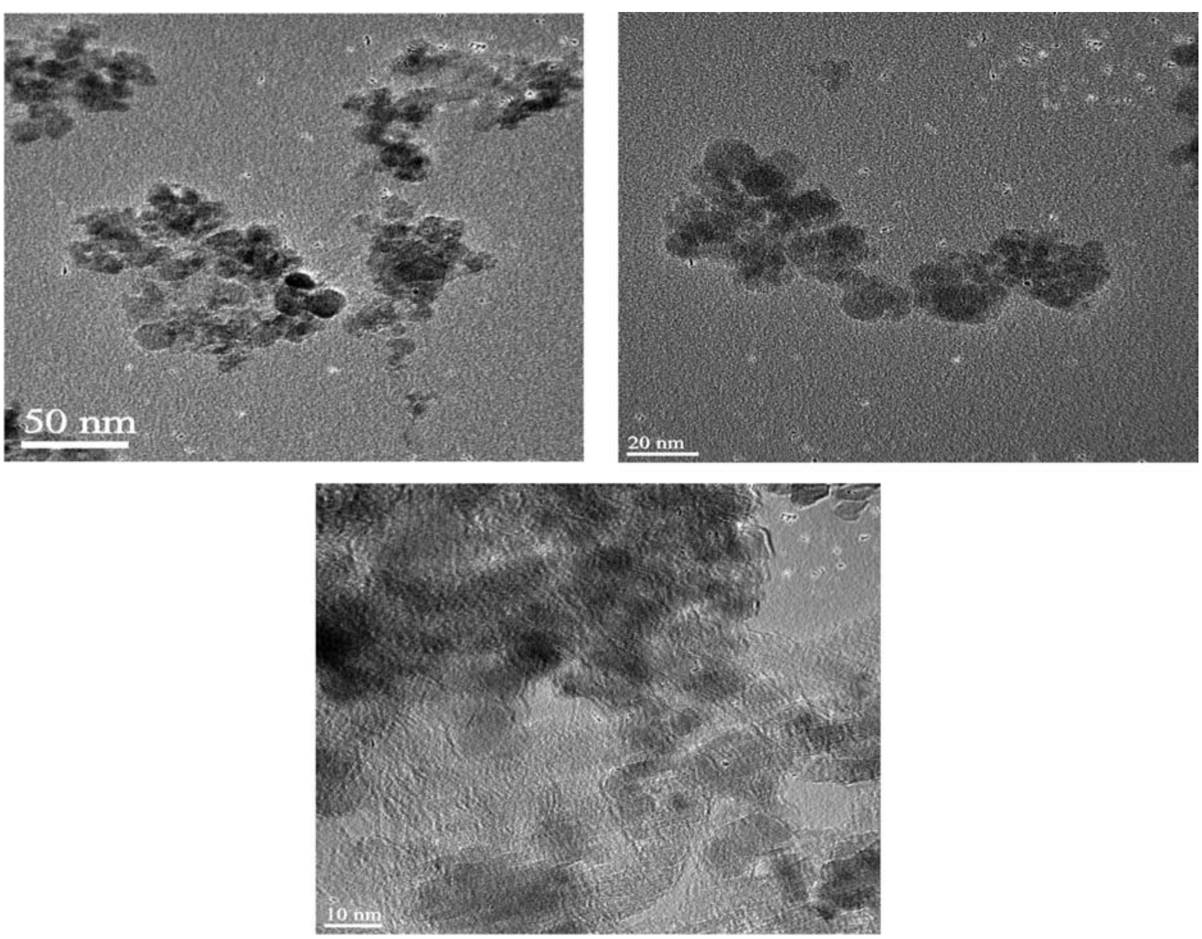

Figure 4. Comparison of TEM and HR-TEM images of C_{60}-γ-Fe_2O_3 SPIONs.

3400 cm^{-1} assigned to the O-H stretching vibration indicated that there were still some -OH groups that had not yet reacted on the surface of the γ-Fe_2O_3 nanoparticles. The peaks at about 630, 590, and 440 cm^{-1} of γ-Fe_2O_3 corresponded to the metal-oxygen vibrational modes of the spinel compounds and are in agreement with the data in the literature (Pereira et al. 2010, Ganachari et al. 2012). Peaks at about 525, 575, 1180, and 1426 cm^{-1} region corresponded to fullerene peaks (Mukhopadhyay et al. 2001). The distinct band 1426 cm^{-1} in Figure 1b. was assigned to C = C vibrations and the band at 1170 cm^{-1} was attributed to C-H in-plane bending vibrations (Barszcz et al. 2007). The peaks at approximately 1400 cm^{-1} and 1600 cm^{-1} observed in curves (a), (b), and (c) indicated a complex reaction between hydroxyl groups on the surface of magnetic nanoparticles. The clarity of the FTIR spectra and the absence of characteristic peaks of C_{60} and γ-Fe_2O_3 were evaluated as coating of γ-Fe_2O_3 with C_{60} as demonstrated in Figure 1c.

XRD patterns of C_{60}-γ-Fe_2O_3 magnetic nanoparticles are presented in Figure 2. The XRD peaks of the C_{60}-γ-Fe_2O_3 were compared with those reported in the literature and spectral library of instrument (Maghemite-Q, Card No. 25-1402). A series of characteristic peaks at $2\theta = 30.5°$, 35.8°, 43.8°, 54.2°, 57.7°, and 63.2°, correspond to (220), (311), (400), (422), (511), and (440) Bragg reflection, respectively. These were in agreement with standard maghemite (γ-Fe_2O_3) XRD patterns (Reddy et al. 2002). However, it was difficult to distinguish the two phases simply from XRD patterns since the XRD patterns of γ -Fe_2O_3 and Fe_3O_4 are reportedly very similar (Ganachari et al. 2012). Peaks at $2\theta = 14.5°$, 18.2°, and 27.4° correspond to pristine C_{60}. The data are in good agreement with that reported in literature (Oh et al. 2007, Baker et al. 2008, Sathish and Miyazawa 2012). These XRD data seem to confirm the coating of γ-Fe_2O_3 with C_{60}.

The microstructure and morphology of C_{60}-γ-Fe_2O_3 magnetic nanoparticles were evaluated by SEM and HR-TEM images. SEM images of C_{60}-γ-Fe_2O_3 magnetic nanoparticles are demonstrated on different resolutions in Figure 3 and the surface morphology analysis demonstrated that it had uniform size distribution. According to the SEM images, the agglomeration was strong in the bare γ-Fe_2O_3 nanoparticles. The agglomeration could be due to the Van der Waals force between the particles and the moisture in sample. Nearly spherical nanoparticles were observed from SEM images. TEM images of C_{60}-γ-Fe_2O_3 magnetic nanoparticles at different resolutions are presented in Figure 4. The main nearly spherical structures of SPIONs are clearly seen. From the TEM images it is clearly observed that particle size is

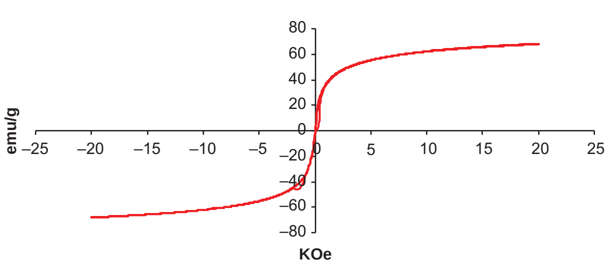

Figure 5. VSM magnetization curve of C_{60}-γ-Fe_2O_3 SPIONs.

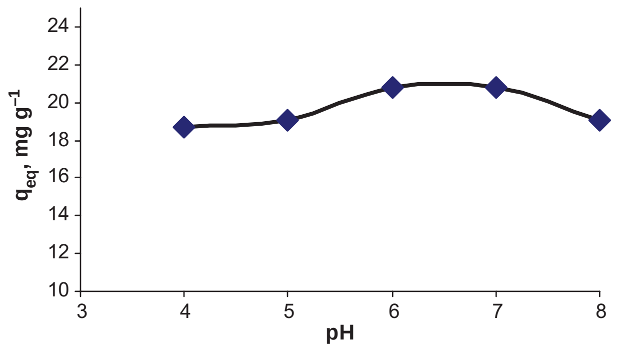

Figure 6. Effect of pH on adsorption of flurbiprofen on C_{60}-γ-Fe_2O_3 SPIONs.

lower than 10 nm. It should be noted that particle size of C_{60}-γ-Fe_2O_3 magnetic nanoparticles makes them usable and removable *in vivo* through extravasation and renal clearance (Gupta and Wells 2004). C_{60}-γ-Fe_2O_3 SPIONs present further functionalization through the targeted drug delivery and specific applications.

The magnetic properties of magnetic nanoparticles were analyzed by VSM. Magnetization curve is presented in Figure 5. The magnetic saturation value of C_{60}-γ-Fe_2O_3 was equal to 66.5 emu g^{-1} which was significantly lower than that for the reported multidomain bulk particles (74 emu g^{-1}) (Shafi et al. 2002). This was attributed to decrease in particle size from 100 nm to < 20 nm ranges and to the coating on surface of γ-Fe_2O_3 with C_{60} (Morales et al. 1997). The result revealed no remanence effect, reflecting superparamagnetic behavior of C_{60}-γ-Fe_2O_3. Additionally, it is clear from high magnetic saturation value that synthesized SPIONs could be useful for biomedical application. Taken together, these data confirm that magnetic nanoparticles composed of γ-Fe_2O_3-C_{60} SPIONs were successfully prepared.

Adsorption of flurbiprofen on C_{60}-γ-Fe_2O_3

Effect of pH on the adsorption on C_{60}-γ-Fe_2O_3 was investigated in the pH range of 4.0–8.0. Fifty mL of flurbiprofen solution at 5.0 µg mL^{-1} concentration was added to 20.0 mg of C_{60}-γ-Fe_2O_3. pH of the aqueous solutions were adjusted to desired value by adding NaOH and HNO_3. After adsorption, SPIONs were magnetically removed. Maximum adsorption

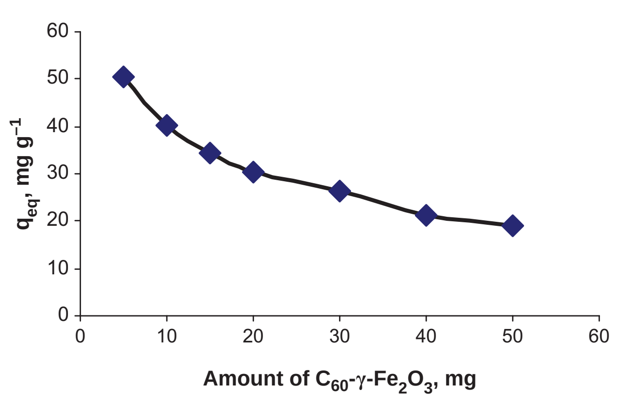

Figure 7. Effect of amount of C_{60}-γ-Fe_2O_3 SPIONs on the adsorption of flurbiprofen.

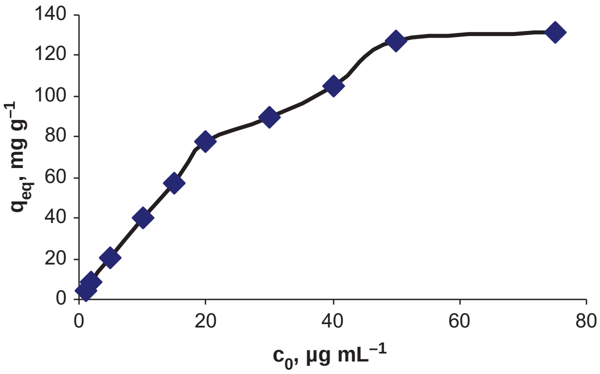

Figure 8. Effect of initial concentration of flurbiprofen on the adsorption on C_{60}-γ-Fe_2O_3 SPIONs on the adsorption of flurbiprofen.

was observed at approximately pH 6.0. Results are presented in Figure 6. Effect of amount of SPIONs was also investigated in the ranges of 5.0–50.0 mg of C_{60}-γ-Fe_2O_3. As shown in Figure 7, higher adsorption values were achieved by lowering in SPIONs amount. Effect of initial concentration of flurbiprofen on the adsorption was investigated in the concentration ranges of 1.0–75.0 µg mL^{-1} of flurbiprofen. As shown in Figure 8 saturation on the surface of SPIONs was observed at approximately 50 µg mL^{-1} of flurbiprofen. Results from adsorption experiments were applied to Langmuir and Freundlich isotherms. By considering the correlation coefficients, it could be said that adsorption results well fitted to Langmuir isotherm. From the plot of c_{eq}/q_{eq} (where c_{eq}: equilibrium flurbiprofen concentration, q_{eq}: mg adsorbed flurbiprofen on per gram of C_{60}-γ-Fe_2O_3) to c_{eq}, equation of curve was obtained as $y = 0.007x + 0.0335$, with coefficient of $r^2 = 0.9922$. From Langmuir equation, as, maximum adsorption capacity was 142.9 mg g^{-1} while K_b was 0.208 L mg^{-1}, it could be concluded that C_{60}-γ-Fe_2O_3 had high surface area. Monolayer adsorption of flurbiprofen on SPIONs could be valid for adsorption of flurbiprofen on C_{60}-γ-Fe_2O_3. Maximum adsorption capacity of C_{60}-γ-Fe_2O_3 was calculated as 142.9 mg g^{-1} (pH of the solution was 6.0, 20.0 mg of C_{60}-γ-Fe_2O_3) from Langmuir isotherm.

Conclusion

The aim of this study was to synthesize and characterize the C_{60} and iron oxide based magnetic nanoparticles with possible application in nanobiotechnology. Secondly, its application in analytical and bioanalytical studies was also investigated. Limitations in the structural and biological compatibility of SPIONs could be overcome by chemical functionalization with carbon based materials such as fullerene. FT-IR, VSM, XRD, SEM, and TEM data confirmed the structure and nanocrystalline nature of the synthesized magnetic particles. The results obtained from this study were expected to give an insight for synthesis and application of C_{60}-γ-Fe_2O_3 magnetic nanoparticles in nanobiotechnology and nanomedicine through *in vitro* and *in vivo* studies. It was observed that synthesized SPIONs were nearly completely spherical structure that contains γ-Fe_2O_3 core C_{60} shell. Adsorption of flurbiprofen on C_{60}-γ-Fe_2O_3 was examined with details. It was found that monolayer adsorption of drug on SPIONs was valid from Langmuir isotherms. By considering the potential applications of C_{60} functionalized SPIONs, further investigations are needed to investigate the applicability, toxicity etc.

Declaration of interest

The author reports no declaration of interest. The author alone is responsible for the content and writing of the paper.

The present work was carried out under the financial support of Mardin Artuklu University) (MAÜ-BAP-14-SHMYO-09).

References

Bae H, Lee K, Lee Y. 2006. Enantioselective properties of extracellular lipase from *Serratia marcescens* ES-2 for kinetic resolution of (S)-flurbiprofen. J Mol Catal B-Enzym. 40:24–29.

Baker GL, Gupta A, Clark ML, Valenzuela MR, Staska LM, Harbo SJ, et al. 2008. Inhalation toxicity and lung toxicokinetics of C_{60} fullerene nanoparticles and microparticles. Toxicol Sci. 101:122–131.

Barszcz B, Bogucki A, Laskowska B, Ion RM, Graja A. 2007. Spectral investigations of fullerene{porphyrin complexes. Acta Phys Pol A. 112:143–152.

Berry CC, Curtis ASG. 2003. Functionalisation of magnetic nanoparticles for applicatiotions in biomedicine. J Phys D Appl Phys. 36: 198–206.

Brettreich M, Burghardt S, Bottcher C, Bayerl T, Bayerl S, Hirsch A. 2000. Globular amphiphiles: membrane-forming hexaadducts of C_{60}. Angew Chem Int Ed. 39:1845–1848.

Daroczi B, Kari G, McAleer MF, Wolf JC, Rodeck U, Dicker AP. 2006. *In vivo* radioprotection by the fullerene nanoparticle DF-1 as assessed in a Zebrafish model. Clin Cancer Res. 12:7086–7091.

Donadel K, Felisberto MDV, Favere VT, Rigoni M, Batistela NJ, Laranjeira MCM. 2008. Synthesis and characterization of the iron oxide magnetic particles coated with chitosan biopolymer. Mater Sci Eng C. 28:509–514.

Enes RF, Farinha ASF, Tome AC, Cavaleiro JAS, Amorati R, Petrucci S, Pedulli GF. 2009. Synthesis and antioxidant activity of [60]fullerene-flavanoid conjugates. Tetrahedron. 65:253–262.

Ganachari SV, Joshi VK, Bhat R, Deshpande R, Salimath B, Rao NVS, Venkataraman A. 2012. Large scale synthesis and characterization of γ-Fe_2O_3 nanoparticles by self-propagating low temperature combustion method. Int J Sci Res. 1:77–79.

Gao J, Gu H, Xu B. 2009. Multifunctional magnetic nanoparticle: design, synthesis and biomedical applications. Account Chem Res. 42:1097–1107.

Gupta AK, Wells S. 2004. Surface-modified superparamagnetic nanoparticles for drug delivery: preparation, characterization, and cytotoxicity studies. IEEE Trans Nanobioscience. 3:66–73.

Hinz B, Brune K, Rau T, Pahl A. 2001. Flurbiprofen enantiomers inhibit inducible nitric oxide synthase expression in RAW 264.7 macrophages. Pharm Res. 18:151–156.

Huang P, Li Z, Lin J, Yang D, Gao G, Xu C, et al. 2011. Photosensitizer-conjugated magnetic nanoparticles for *in vivo* simultaneous magnetofluorescent imaging and targeting therapy. Biomaterials. 32: 3447–3458.

Isobe H, Nakanishi W, Tomita N, Jinno S, Okayama H, Nakamura E. 2006. Nonviral gene delivery by tetraamino fullerene. Mol Pharm. 3:124–134.

Kievit FM, Zhang M. 2011. Surface engineering of iron oxide nanoparticles for targeted cancer therapy. Account Chem Res. 44:853–862.

Kilinc E, Aydin F. 2009. Stability-indicating HPTLC analysis of flurbiprofen in pharmaceutical dosage forms. J Planar Chromat. 22:349–354.

Kilinc E, Aydin F. 2012. Optimization of continuous flow hydride generation inductively coupled plasma optical emission spectrometry for sensitivity improvement of bismuth. Anal Lett. 45: 2623–2636.

Kroto HW, Heath JR, O'Brien SC, Curl RF, Smalley RE. 1985. C_{60}: Buckminsterfullerene. Nature. 318:162–163.

Lee EG, Won HS, Ro H, Ryu Y, Chung BH. 2003. Preparation of enantiomerically pure (S)-flurbiprofen by an esterase from *Pseudomonas* sp. KCTC 10122BP. J Mol Catal B Enzym. 26:149–156.

Liu X, Ma Z, Xing J, Liu H. 2004. Preparation and characterization of amino-silane modified superparamagnetic silica nanospheres. J Magn Magn Mater. 270:1–6.

Meng Z, Zhang F, Zhu L, Park C, Ghosh T, Choi J, Oh W. 2012. Synthesis and characterization of M-fullerene/TiO_2 photocatalysts designed for degradation azo dye. Mater Sci Eng C. 32:2175–2182.

Morales MP, Serna CJ, Bodger F, Morup SJ. 1997. Spin canting due to structural disorder in maghemite. J Phys Condens Matter. 9: 5461–5468.

Mukhopadhyay K, Dwivedi CD, Mathur GN. 2001. Quality assessment of fullerene samples using thermal technique. J Therm Anal Calorim. 64:765–771.

Mroz P, Pawlak A, Satti M, Lee H, Wharton T, Gali H, et al. 2007. Functionalized fullerenes mediate photodynamic killing of cancer cells: Type I versus Type II photochemical mechanism. Free Radic Biol Med. 43:711–719.

Nakamura E, Isobe H, Tomita N, Sawamura M, Jinno S, Okayama H. 2000. Functionalized fullerene as an artificial vector for transfection. Angew Chem Int Ed. 39:4254–4257.

Netto CGCM, Toma HE, Andrade LH. 2013. Superparamagnetic nanoparticles as versatile carriers and supporting materials for enzymes. J Mol Catal B Enzym. 85–86:71–92.

Oh W, Jung A, Ko W. 2007. Preparation of fullerene/TiO2 composite and its photocatalytic effect. J Ind Eng Chem. 13:1208–1214.

Partha R, Mitchell LR, Lyon JL, Joshi PP, Conyers JL. 2008. Buckysomes: fullerene-based nanocarriers for hydrophobic molecule delivery. ASC Nano. 2:1950–1958.

Partha R, Conyers JL. 2009. Biomedical applications of functionalized fullerene-based nanomaterials. Int J Nanomed. 4:261–275.

Pereira C, Pereira AM, Quaresma P, Tavares PB, Pereira E, Araújo JP, Freire C. 2010. Superparamagnetic γ-Fe_2O_3@SiO_2 nanoparticles: a novel support for the immobilization of [VO(acac)2]. Dalton T. 39:2842–2854.

Pignatello R, Bucolo C, Spedalieri G, Maltese A, Puglisi G. 2002. Flurbiprofen-loaded acrylate polymer nanosuspensions for ophthalmic application. Biomaterials. 23:3247–3255.

Reddy CVG, Cao W, Tan OK, Zhu W. 2002. Preparation of $Fe_2O_{3(0.9)}$–$SnO_{2(0.1)}$ by hydrazine method: application as an alcohol sensor. Sensors Actuator B. 81:170–175.

Sathish M, Miyazawa K. 2012. Synthesis and characterization of fullerene nanowhiskers by liquid-liquid interfacial precipitation: influence of C_{60} solubility. Molecules. 17:3858–3865.

Satoh M, Takayanagi I. 2006. Pharmacological studies on Fullerene (C_{60}), a novel carbon allotrope and its derivates. J Pharmacol Sci. 100:513–518.

Shafi KVPM, Ulman A, Dyal A, Yan X, Yang N, Estournes C, et al. 2002. Magnetic enhancement of γ-Fe_2O_3 nanoparticles by sonochemical coating. Chem Mater. 14:1778–1787.

Sorge AA, Delft JL, Bodelier VMW, Wijnen PH, Haeringen NJ. 1998. Specificity of flurbiprofen and enantiomers for inhibition of prostaglandin synthesis in bovine iris/ciliary body. Prostag Oth Lipid M. 55:169–177.

Stanciu L, Won Y, Ganesana M, Andreescu S. 2009. Magnetic particle-based hybrid platforms for bioanalytical sensors. Sensors. 9:2976–2999.

Tóth E, Bolskar RD, Borel A, Gonzalez G, Helm L, Merbach AE, et al. 2005. Water-soluble gadofullerenes: toward high-relaxivity, pH-responsive MRI contrast agents. J Am Chem Soc. 127:799–805.

Veiseh O, Gunn JW, Zhang M. 2010. Design and fabrication of magnetic nanoparticles for targeted drug delivery and imaging. Adv Drug Deliver Rev. 62:284–304.

Yigit MV, Moore A, Medarova Z. 2012. Magnetic nanoparticles for cancer diagnosis and therapy. Pharm Res. 29:1180–1188.

Yiu HHP, Keane MA. 2012. Enzyme-magnetic nanoparticle hybrids: new effective catalyst for the production of high value chemicals. J Chem Technol Biotechnol. 87:583–594.

Zhang LW, Yang J, Barron AR, Monteiro-Riviere NA. 2009. Endocytic mechanisms and toxicity of a functionalized fullerene in human cells. Toxicol Lett. 191:149–157.